Chinese Chemical Letters 34 (2023) 107819

Contents lists available at ScienceDirect

Chinese Chemical Letters

journal homepage: www.elsevier.com/locate/cclet

3D skin models along with skin-on-a-chip systems: A critical review

Wenxuan Sun[a], Zijia Liu[a], Jian Xu[b], Ya Cheng[b], Ruixue Yin[a], Lei Ma[c], Honglin Li[c], Xuhong Qian[c,d], Hongbo Zhang[a,*]

[a] School of Mechanical and Power Engineering, East China University of Science and Technology, Shanghai 200237, China
[b] School of Physics and Electronic Science, East China Normal University, Shanghai 200062, China
[c] School of Pharmacy, East China University of Science and Technology, Shanghai 200237, China
[d] School of Chemistry and Molecular Engineering, East China Normal University, Shanghai 200062, China

ARTICLE INFO

Article history:
Received 29 June 2022
Revised 2 September 2022
Accepted 9 September 2022
Available online 13 September 2022

Keywords:
3D skin model
Skin equivalent
Skin-on-a-chip
3D bioprinting
Skin barrier

ABSTRACT

Skin is the largest organ in human body, and it plays an important role in regulating physiological microenvironments and acts as a barrier to protect human body from harmful intrusions. The demand for fully functional skin models (also called skin equivalents, SE) in an *in-vivo* mimicking culturing microenvironment has been increased dramatically due to the fast development in skin disease treatments and skin care products. Owing to the emerging of the concept and technology of organ-on-chips along with the three-dimensional (3D) bioprinting technology, 3D skin models and their applications have been fast evolving. In this paper, the advances in the development of 3D skin models along with skin-on-a-chip (SOC) are reviewed and commented. One of the findings with this paper is that the SOC together with the 3D bioprinting technology is promising to construct fully functional 3D skin models in the field of pharmaceutical and cosmetic industries.

1. Introduction

Human skin plays an important role in protecting human body, regulating body temperature and sensing external stimuli. Human skin has three distinct layers with two main types of cells: (i) the adipose rich hypodermis, (ii) the dermis with fibroblasts (FBs)-penetrated in collagen populated extracellular (ECM), and (iii) the stratified squamous epidermis consisting primarily of keratinocytes (KCs). Other important features of skin include blood vessels, hair follicles, sweat glands, muscle, and nerves. Although the skin structure is simple, however, fully functional 3D skin models are not commercially available yet. Development of effective therapies for skin diseases and testing of skin care products have driven the development of the so-called fully functioning 3D SOC models or systems. This is particularly urgent with the ban in animal test for skincare products in Europe [1].

Currently, commercially available skin models are fabricated mainly using collagen as a substrate by feeding a recipe of growth factors at different periods in transwell or petridish [2–4]. The main difficulties of creating 3D models are: (1) the formation of epidemies, which require strict selections of sources of cells and feeding of active factors; (2) the culturing time is limited due to the static culturing conditions; (3) the dermis and epidermis junction (DEJ) is often incomplete, therefore hinders skin functions.

In recent years, organ-on-a chip (OOC) that combines tissue engineering and microfluidic technology has been developed rapidly [5–7]. Due to the fine control of microfluidics, the cellular differentiation, cell-cell and cell-matrix interactions are improved compared to static culture. The unique advantages of the SOC in the 3D cell culture overcome the limitation of the traditional 2D skin models, which lack the complex physiological functions of human tissues and organs [8,9]. OOC technology has also been applied to construct human skin models [10,11].

In this paper, the advances in the development of 3D skin models especially their applications to SOC, fabricated with 3D bioprinting, are reviewed and commented. The functions of 3D skin model are of great importance in drugs and cosmetic ingredient screening, and disease modeling. The key properties of skin, such as barrier functions and how to measure the key features are also discussed.

2. Fabrication methods of 3D skin models

2.1. 3D bioprinting

3D bioprinting is a new field in regenerative medicine. In 3D bioprinting, a printer is controlled by a computer to accurately

* Corresponding author.
E-mail address: hbzhang@ecust.edu.cn (H. Zhang).

https://doi.org/10.1016/j.cclet.2022.107819
1001-8417/

deposit bioinks consisting of living cells, biological materials, and other biological substances in a layer-by-layer fashion, providing a suitable environment for cell migration, proliferation and differentiation simulating various tissues of human body. It not only has high potential in tissue regeneration, but also plays an important role in drug delivery, cancer research, *etc.* [12,13]. It is extremely beneficial in patient-specific treatments, not only in creating patient specific tissue structure and microenvironment, but also in patient specific types of cells [14].

As one of the application areas of 3D bioprinting, skin bioprinting has attracted much attention in recent years. There is a growing demand for artificial skin in drug testing, disease research and cosmetic testing [15,16]. It is of a great challenge to obtain tissue engineered skin that can mimic skin biomechanical properties. The 3D printing methodology along with bioinks is the key to successfully construct artificial skin models.

2.1.1. Methodology

3D bioprinting can be categorized into two main types: extrusion-based and photocuring-based. The comparison of various methods is summarized in Table S1 (Supporting information).

(1) Extrusion-based bioprinting has been available for a while on the market. It mainly utilizes various physical methods to push the bioink from a nozzle onto a substrate, thus forming a 3D structure. It is mainly divided into extrusion, inkjet and laser assisted printing.

Extrusion is currently the most studied and widely used bioprinting [17], According to the way of obtaining power, it can be divided into pneumatic method, piston method and screw method [18]. The bioink, which can be used in extrusion bioprinting, has a wide range of viscosity with high cell density. However, extrusion technology also has some drawbacks. For example, when the viscosity of bioink is too high, it causes higher the shear stress resulting in a low cell survival rate [19]. And the resolution and precision of extrusion bioprinting is also limited [20].

Inkjet printing is developed from traditional 2D bioink jet printing. This printing technique can be divided into thermal inkjet printing and piezoelectric inkjet printing [21]. Piezoelectric printing utilizes piezoelectricity to generate sound waves, driving bioink through a micro nozzle to form the desired pattern [22]. The limitation of this method is that the viscosity weakens the applied acoustic/pressure wave, thus hindering the spray of droplets. Therefore, it is impossible to use high-concentration and viscous bioinks [23]. In addition, the printed cell density is relatively low.

Laser-assisted bioprinting (LaBP) utilizes laser pulse to the absorption layer, forming microbubbles or vapors and resulting in shock waves to deposit bioink [24]. The nozzle of LaBP is simple, therefore, there is no nozzle clogging due to its non-contact nature, however, its printing efficiency is low and the laser energy input might cause thermal damage to cells [25,15].

(2) Photocuring-based bioprinting is based on the photopolymerization of photosensitive polymers under precisely controlled lighting. Compared with other bioprinting methods, it usually has a higher resolution and printing speed. In addition, there is no concern about nozzle blockage and shear stress affecting cell viability [26], however, when a laser is used, it may damage cells. According to the light scanning process, Photocuring-based bioprinting can be divided into stereo lithography (SLA) and digital light procession (DLP).

In SLA laser scans the surface of bioink, photon absorption generates 2D patterns [27], after each layer is completed, the manufacturing platform moves in z direction to form a new layer [28]. SLA has a few advantages, such as low or no shear stress, high cell viability and a wide range of bioink selection. However, ultraviolet radiation might cause cell damages [29]. Unlike SLA, DLP solidifies a complete layer at one time rather than point by point. The principle is to use UV or visible light curing photosensitive polymer in a layer-by-layer fashion with top-down or bottom-up settings. Compared with the other bioprinting methods, it has many merits: DLP allows layer-by-layer aggregation and the printing time for each layer is the same, regardless of complexity or size, depending only on the thickness of the structure [30]. This nozzle-free approach also leads to a very high cell viability (85%–95%) and prevents clogging at high cell density [22].

2.1.2. Bioink

Bioink is a mixture of cells and biomaterials that has specific properties for bioprinting of live tissues [31]. Firstly, high cell survival rates, good biocompatibility are required. Secondly, sufficient mechanical properties are needed to ensure high-precision and high-quality structures, therefore, appropriate rheological properties are required. The biological materials used in bioinks can be divided into natural materials, synthetic materials [15]. Natural materials, including collagen, gelatin, fibrin, sodium alginate, chitosan and hyaluronic acid, have similar biological activities to normal skin tissues and can support cell migration, proliferation and differentiation. The synthetic materials are produced by chemical synthesis, such as polylactic acid, polycaprolactone, polyethylene glycol and its derivatives, the advantage is that it can be mass-produced by industrial methods with good mechanical properties. However, the biological characteristics need to be improved. The biomaterials used in bioprinting of skin models are summarized in Table S2 (Supporting information).

2.1.3. 3D bioprinting of skin tissue

(1) Multilayer skin structure printing

3D bioprinting is ideal for creating skin models, which have a distinctive stratified feature [32,33]. Lee *et al.* [34] printed skin models, which consist of six layers of collagen, three layers of FBs and two layers of collagen alternately, separating the stacked FBs layer from the KCs. It can be observed that the top layer is dense and denser over time. The dermis is sparse showing obvious contraction and compaction over time. However, the epidermis is less than 50 μm, the main reason might be that the dense layers of collagen hinder the nutrition reaching to the internal parts of the artificial structures.

(2) Full thickness skin model construction.

Ramasamy *et al.* [35] created full thickness skin model *via* 3D biprinting of FBs and KCs onto 3D printed porous PCL scaffolds, which ensured sufficient nutrition supply. The epidermis has a distinctive basal layer, spinous layer, granular layer and cuticle, similar to human skin. The keratin K14 and K10 were expressed in the lower and upper layer of the stratified epidermis. The basal layer showed occasional Ki67 positive cells, indicating the presence of proliferation cells. Laminin V and collagen IV are the key components of DEJ, which provides an anchor between epidermis and underlying dermis and plays a good barrier role [36]. This research shows that 3D bioprinting could offer and promote the synthesis and deposition of basement membrane components by prolonging the integrity of dermal matrix, which helped the whole skin equivalent function.

Jin *et al.* [37] printed 3D skin constructs using inkjet printing with emphasis on the role of calcium ions, which plays an important role in HaCaT cell differentiation [38]. The skin structure was stabilized for 2 days by liquid-liquid interface (LLI), then gas-liquid interface (ALI) culture was applied for keratinization. The optimum conditions of keratinization were obtained by varying the calcium ion concentration for 14 days and then the keratinization of printed skin was observed histologically. This is a process of forming epidermal barrier, resulting in the production of various types of cytokeratins [39]. In addition, loricrin (LOR) is one of the

components of consistent cell membrane and is used as a molecular marker for terminally differentiated epidermal cells during keratinization [40]. The results showed that the expression of LOR and CK14 was increased after ALI in the printed 3D full thickness skin model.

Kim *et al*. [41] bioprinted a 3D full thickness human skin model with combined printing methods. Extrusion printing module is used to print 3D dermal compartment, where human dermal fibroblasts (HDFs) were encapsulated in skin-derived extracellular matrix (S-dECM) bioink. During the 45-min crosslinking period, human epidermal keratinocytes (HEKs) were evenly distributed in the dermal chamber by the inkjet printing module. The results showed that dECM-based 3D skin models encapsulating endothelial progenitor cells (EPCs) together with adipose-derived stem cells (ASCs) significantly improved the angiogenesis and reperfusion-epithelialization and wound closure.

(3) Skin structure with melanin

Melanocytes are important cells in epidermis, this type of cells is relevant to most of skin diseases, and regulates the epidermal microenvironment [42]. Pigmented human skin model is regarded as the models that add melanin cells to the skin structure with pigmentation like that of human skin.

Ng *et al*. [43] constructed a pigment skin model, it was found that when cells were cultured in the early stage, different proportions of mixed co-culture medium would affect the proliferation of cells. The results showed that with the increase of the ratio of keratinocyte growth medium (KGM) and melanocyte growth medium-M2 (MGM), the growth rate of FBs decreased, and the growth rate of melanocytes slowed down. KCs were highly sensitive to the changes of medium. In addition, a key aspect of skin pigmentation is the transfer of melanocytes from melanocytes to KCs. It is very important to provide the optimal KCs density for proliferation and differentiation into well stratified epidermis. Shi *et al*. [44] constructed a 3D skin model with precisely control over the number and location of melanocytes in epidermis. It was found that the uptake of melanosomes is highly dependent on the differentiation of KCs [45].

Compared with the manual casting method, the cell distribution at the top of the dermal region and the microstructure in the dermal region were significantly different. Bioprinting technology helps to control the pore size in the 3D collagen matrix with FBs to produce hierarchical porous structures similar to that of natural skin tissues. Uneven skin pigmentation was observed in the artificially cast 3D colored human skin. The pigment deposition in 3D bioprinted skin structure is uniform and melanin particles are evenly distributed in the epidermis [44]. The human skin structure was stained to determine the expression of collagen VII, HMB-45, keratin 1 and keratin 6. All antibodies showed positive in the 3D bioprinted skin structure, while only HMB-45 and K6 showed positive staining in the manual casting skin structure. The continuous collagen VII protein can be observed in the 3D bioprinted skin structure, but only the trace of col VII can be detected in the manual casting skin structure. This indicates that there is a thin VII collagen layer at the interface between epidermis and dermis in the printed structure, and a well-developed stratified KCs layer exists in the outermost layer of the epidermis region, while most of the epidermis regions of the manual casting skin structure lacks differentiated KCs [45].

2.2. SOC

SOC is to culture and evaluate skin tissues in a microfluidic system. SOC integrates all components such as sample preparation, reaction, separation, analysis and detection to complete biological and chemical reactions, analysis, and real-time detection [46]. The system can control physical and biochemical parameters such as medium flow, mechanical force and biochemical gradient to simulate the 3D microenvironment of natural human skin [47], and multi-cell 3D culture can be realized by multi-channel configurations.

In SOC, cells usually grow on the surface of microcavities or porous membranes, and a continuous perfusion medium is supplied through microchannels (normally, a few hundred micros in size), the medium flows from one chamber to another by gravity, capillary drive or active pumps. The continuous flowing media in the lower layer can simulate the blood flow in blood vessels, while keeping the cells in a healthy state, preventing the accumulation of metabolic wastes and providing the necessary fluid shear stress [3].

The microenvironment, monitoring parameters and applications required for cell function determine the choice of chip materials which are related to manufacturing techniques, stimuli required and interface layouts [4]. Material selection must take into account the creation of appropriate culture chambers and fluid connections, induction forces and stiffness to reconstruct biological functions, and potentially increase electrical stimulation and braking to control and observe the created biological tissue models [48]. Common used materials include silicone elastomers, such as polydimethylsiloxane (PDMS), glass and thermoplastic polymers such as polystyrene (PS), polycarbonate (PC) and polymethyl methacrylate (PMMA). These materials are optically transparent and have good biocompatibility suitable for observing and performing various cell-based analysis [49]. Among these materials, PDMS is very popular because of its low manufacturing cost, good transparency, air permeability, easy handling, efficient sealing process and easy formation of complex micropatterns [50]. In addition, patterns can be transferred to multiple substrates made of glass, elastomeric polymers and plastics [51,52].

A wide variety of skin models has been created by SOC. The skin models created by SOC can be divided into two categories according to the skin structures in the model: 2D models in which cells are directly attached to the membrane and 3D skin structures.

2.2.1. 2D skin models by SOC

Skin models made on 2D porous membrane are usually simple and easy to create. In these 2D models, the membrane is often used as the dermal layer because of its good permeability. Table S3 (Supporting information) gives a summary of the skin models created on membranes.

Ramadan and Ting [53] also introduced dendritic cells (DCs) into their model, in which KCs and DCs were co-cultured and separated by a porous membrane. These two types of cells represent the epidermal layer of the skin and the subcutaneous immune system, respectively. This research also showed that perfusion-based cell culture promotes skin barrier functions and prolong the lifespan of cellular system. The barrier role of KCs was analyzed by applying LPS to HaCaT, U937 and HaCaT/U937, respectively, TEER was also tested. The results showed that the KCs form a strong barrier to the invasion of endotoxins. This SOC can be used as a powerful tool for skin sensitization and toxicity tests. Sasaki *et al*. [54] developed a SOC for parallel permeation assays. The Permeation assays were observed with $K_2Cr_2O_7$ comparing with FITC-Dex solution. This research shows that SOC has the potential for drug development.

Wufuer *et al*. [55] developed a human SOC model consisting of three layers, epidermal, dermal and vascular layer for the first time in the aim to study inflammation and edema. The three layers were represented by HaCaT, FBs, and HUVEC cells, respectively, and separated by transparent porous membranes to allow interlayer communication and mimic skin biology.

2.2.2. 3D skin models by SOC

The 3D skin equivalent is either directly taken from biopsy or obtained by seeding cells. Table S4 (Supporting information) summarizes the 3D skin models from biopsies cultured on SOC, and Table S5 (Supporting information) is a summary of skin equivalent obtained by casting on SOC.

(1) Skin biopsies using in SOC and multi-organ co-culture (MOC) chips

Ataç *et al.* [56] used the SOC to culture follicular unit extracts (FUEs) as a further step in an attempt to emulate the biology of skin and its appendages. In this work hair follicles and skin tissue were co-cultured in transwell both in static and dynamic perfusion conditions in the aim to prolong the culture period of the *ex vivo* hair follicles, taking into account the support of glands and surrounding skin tissue on hair follicle maintenance. The results indicate that there is a distinct difference between the static and MOC culturing condition, and the tissue disintegration was also prevented by dynamic perfusion. Bajza and his team [57] committed a research of transdermal drug delivery. They designed and fabricated a novel temperature-controlled microfluidic device for testing drug penetration through the skin. Skin tissues cultured in a microfluidic device were compared with the Franz diffusion cell system to investigate drug diffusion. Microdialysis technology was utilized for the continuous monitoring of unbound analyte concentrations in the extracellular milieu in different tissues. The result showed that their device provides similar information on the characteristics, degree, and speed of absorption of the test drug (caffeine) through the dermal barrier. Their model could serve as a new approach for the investigation of skin penetration and transporter interactions at dermal barrier.

Skin tissue from biopsies is often used in MOCs, which establish specific multi-organ systems, such as a circulatory system, intestine systems, which are often used to study drug metabolism. Wagner *et al.* [58] established a liver-skin co-culture system for drug toxicity test. In perfusion culturing conditions both tissues retained a metabolically active phenotype for up to 28 days. Maschmeyer *et al.* [59] manufactured a MOC to host four human organ equivalents: (i) a reconstructed human 3D small intestine and (ii) a skin biopsy opting for oral and dermal substance absorption, (iii) a 3D liver equivalent enabling primary substance metabolism and (iv) a kidney proximal tubule compartment supporting metabolite excretion. A robust protocol has been established for the co-culture of these four human tissues over at least 28 days. This MOC model enables the evaluation of pharmacokinetics and pharmacodynamics, such as effective concentration, maximum tolerable dose, time course and intensity of therapeutic and adverse effects.

(2) Skin equivalents obtained by seeding cells on SOC

The current research on skin equivalents cultured in SOC mainly focuses on two aspects due to the lack of living skin complex: (1) optimizing 3D skin structure in terms of materials, cell sources, active factors, vasculatures, *etc.* to mimic the biological complexity of *in vivo* skin; (2) ameliorating microfluidic devices to promote epidermal morphogenesis and differentiation.

There were attempts to recapitulate the 3D structure of skin by using various ECM scaffolds including collagen. Type I collagen was the most widely used material as a cell culture scaffold for artificial skin models. Song *et al.* [60] tested collagens from different sources, rat tail, porcine skin, and duck feet, comparing their abilities to support cell growth and differentiation. Among the three collagen sources, the rat tail collagen showed the best result in terms of expression of marker proteins and formation of dermis and epidermis layers. By comparing transwell culture conditions with SOC conditions, they concluded that transwell culture conditions supported the growth and differentiation of skin equivalents better than chip conditions. Therefore, the culture conditions on the chip need to be further optimized.

Jusoh *et al.* [61] studied the angiogenesis responses induced by VEGF upregulation from damaged KCs as an alternative to animal models. KCs were treated with sodium lauryl sulfate (SLS) to obtain upregulated VEGF. The results showed that blood-vessel formation was enhanced by coculturing dermal FBs with quiescent KCs. As an endothelial and microvessel hyperpermeability growth factor, the VEGF secreted by KCs may stimulate vessel formation in angiogenesis due to paracrine communication between endothelial cells and KCs under quiescent conditions. This platform provided a new approach to replace avascular skin-irritation models.

By combining molding and microfluidic technology, Salameh *et al.* [62] developed a fully vascularized perfusable reconstructed skin that comprises a fully differentiated epidermis, perfusable macrovessels with angiogenic sprouts, and a microvascular network with capillaries organized by vasculogenesis in the dermis. In this work nylon threads were used to create hollow vascular structures and generate secondary capillary networks through angiogenesis. Perfusable vasculature with closer proximity to the native vascular plexus provided a more reliable model for local and systemic assessment. Lee *et al.* [63] built a skin chip that has microfluidic channels to enable vascular endothelial cell culture, as well as a chamber for 3D culture of skin cells (FBs and KCs). Gravity was applied to rock the platform for pumpless perfusion. The custom-made gravity device consists of a rotating stage and dish holder, which is controlled by a computer program to adjust the tilting angle and frequency of rotation. This chip maintained culturing condition for up to 2 weeks.

The discovery of induced pluripotent stem cells (iPSCs) in 2006 was a major breakthrough in biomedical science [64]. In 2014, Gledhill *et al.* [65] generated the first Human 3D skin equivalents (HSE) from iPSC-derived KCs, melanocytes and FBs containing a functional iPSC-derived epidermal-melanin unit. It was the first report of 3D skin equivalents generated exclusively from three human iPSC-derived cell types, and the first description of melanin generation and transfer between human iPSC-derived melanocytes and KCs were provided. Their work opened up a new area of research in the source of cells to generate SE.

Most of the microchips used in MOCs and SOCs are made of PDMS. Risueño *et al.* [66] presented a new, cost-effective, robust, vinyl-based microfluidic platform for skin-on-a-chip applications. This platform was produced by micro-machining, which provides more simplicity in the fabrication process, as well as increased flexibility and versatility in the layout of the device, overcoming some of the limitations of PDMS. They also devised a method to simplify the skin structure by introducing parallel flow controlled by a syringe pump for the first time.

Sriram *et al.* [67] presented a novel microfluidic device for integrated culturing and testing of full-thickness human skin equivalents. The device is composed of a non-contracting fibrin-based dermal matrix and a thermoplastic-based chip amenable to mass production. The SE is reconstructed directly on this OOC device that enables permeation and toxicity studies to be conducted. The SEs cultured on-chip were compared with the SEs cultured in the standard tissue culture system. The results showed that the former not only exhibited an improved epidermal differentiation, but also enhanced barrier function and, consequently, lower skin permeability.

3. Skin functions

3.1. Skin barrier

Biological barriers are crucial for the integrity and proper function of various organs [68]. Disruption and dysfunction of barrier-forming tissues are an integral part of the pathophysiology of many disorders such as skin barrier in psoriasis [69]. The skin provides

mechanical protection and is an important barrier against external intrusion and uncontrolled loss of body fluids. Its barrier function is mainly derived from the epidermis, which is a stratified epithelium with a basal layer of proliferating cells and multiple suprabasal layers of differentiated KCs [70]. When building 3D skin models, whether 3D printed models or models from microfluidic chips, one of the difficulties to construct skin models similar to native human skin is the barrier formation. This limits the applicability of skin models on pharmacokinetic and toxicological screening [71]. Therefore, there is an urgent need to form proper skin barrier. The following methods have been used to evaluate barrier function.

3.1.1. Detection of TEER

TEER is a valuable non-invasive technique that can be used to quantify the barrier integrity of cells at their different stages of growth and differentiation [72]. It is particularly useful for monitoring the development of *in vitro* models and their ability to form an effective permeability barrier. These measurements are usually conducted using a commercial instrument EVOM according to the Ohm's first law [73]. TEER has become a widely accepted method to evaluate tissue barrier function *in vitro* [72]. Zoio *et al.* [74] fabricated a low-cost barrier-on-chip (BoC) device with integrated electrodes for the real-time monitoring of biological barriers. The integrated tetrapolar electrode configuration resulted in a more homogenous sensitivity distribution along the culture area compared with conventional chopstick systems. A state-of-the-art full-thickness model (FTSm) was developed inside the BoC by providing a dynamic microenvironment and correctly establishing an ALI. In particular, TEER measurements can be useful to monitor the effect of irritants on biological barriers. Given the flexibility of the platform, additional cell types could be added to the FTSm and other epithelial tissues could be reconstructed and monitored.

3.1.2. Detection of protein expression level

The skin barrier is composed of KCs produced by the differentiation of epidermal KCs, various proteins synthesized and secreted during the differentiation process [75,76]. Differentiation of epidermal KCs plays a very important role in skin barrier function. Although the epidermal barrier function is mainly attributed to the stratum corneum (SC), recent studies have shown that tight junctions (TJs) in the epidermis also play an important role in maintaining barrier function [77]. KCs assemble numerous cytoskeletal filaments that are partially anchored to intercellular junctions such as desmosomes, tight junctions, and adherent junctions, which contribute to the mechanical stability and optimal elasticity of the epithelium. In addition, differentiated KCs secrete lamellar bodies, which also contribute to the formation of skin barrier [70]. The skin barrier can be characterized by detecting related proteins secreted by cells. Therefore, in addition to the detection of TEER, Murakami *et al.* [78] used real-time quantitative PCR and western blotting to detect the gene and protein expression levels of cell differentiation markers such as LOR and transglutaminase (TGase) to evaluate barrier functions.

Tight junction scaffolding proteins in the epidermis include zonula occludens (ZOs) and transmembrane proteins. ZO contributes to the aggregation of transmembrane proteins, such as claudins and occludins, to form tight junctions. ZO-1 is specifically or predominantly expressed at the cellular edge of SGs, whereas claudin-1 is expressed throughout the epithelium. Therefore, Murakami *et al.* [79] applied the immunocytochemical methods and electron microscopy to detect claudin-1 (CLDN1) and ZO-1 to prove that the skin model they designed had a skin barrier. Kubo *et al.* [80] examined the expression of barrier-related proteins at different differentiation stages of epidermal KCs, including pro-filaggrin (FLG), pro-caspase-14 (CASP14), CLDN1, and claudin-4 (CLDN4).

In Pell *et al.*' s work [81] junctional complex protein imaging was used to analyze epithelial barrier integrity. A validated, systematic and scalable 3D quantitative immunofluorescence imaging technique was presented to assess *in situ* barrier integrity within Transwell by analyzing the junctional complex proteins of ZO-1 and occludin. The combination of improved TEER data analysis and automated tight junction protein image analysis allowed for data analysis without the need for blank well correction.

3.1.3. Detection of transepidermal water loss (TEWL)

TEWL, which is defined as the amount of water that enters the body through the epidermis, is considered one of the most important parameters to characterize skin barrier function. The principle is that the water vapor pressure across the epidermal permeability barrier is different, and water will passively evaporate through the skin, and the amount of water lost by skin evaporation is measured to evaluate the state of the skin permeability barrier [82]. Higher level of TEWL were found in damaged skin [83]. Decreased or lower water loss indicates skin barrier integrity or improvement [84]. Murakami *et al.* [78] used the Vaposcan AS-VT100RS to measure the water loss in 3D cultured skin tissues.

3.1.4. Quantitative determination of ceramides

Intercellular lipids in the stratum corneum (SC) include ceramides, cholesterol, and free fatty acids, which provide barrier function by forming a lamellar structure [85]. Among them, ceramides account for about 50% of intercellular lipids, and the rest consists of cholesterol and free fatty acids [86]. Ceramides are composed of sphingosine and fatty acids and have multiple functions. These lipids have been reported to play important roles in promoting KCs differentiation [87], lamellar structure formation, and skin permeability barrier formation. Therefore, measuring ceramide levels can also assess skin barrier [78]. Since epidermal glucosylceramide and ceramide are composed of heterogeneous species, HPTLC is suitable for these lipid analyses [82].

In Murakami *et al*'s. work [78], the ceramides were quantified by HPTLC to access skin barrier function. It was found that the skin barrier function was improved by culturing cells at specific estrogen (*E*) and progesterone (*P*) concentration ratios, which would be considered beneficial for female skin. This suggests that dysregulated *E/P* concentration ratios may be the cause of certain skin problems.

3.1.5. Cell viability assay

The barrier function of skin is also studied by determining the concentration of a benchmark chemical that reduces tissue viability by 50% after a fixed exposure time. Dijkhoff *et al.* [88] used the MTT assay to determine the exposure time required for a 50% reduction in tissue viability. In the latest research [89] a variety of methods to detect the skin barrier function was used. First, the viability of the cells was analyzed by MTT. The sodium dodecyl sulfate (SDS) treated samples were then infiltrated with the dye lucifer yellow (Sigma) and treated with detergent, and the tissue was fixed for sectioning observation to further evaluate the barrier function of the skin model. Finally, it was assessed by monitoring the TEER of the FTSm and reconstructed skin model (RHEm) 12 days after ALI addition.

3.2. Mechanical strength

Tension plays a critical role in the development of organs and tissues, including the establishment of morphological and functional properties. By creating internal tension, the skin plays a vital role in repelling, buffering, and protecting the deep tissue, which includes the lining of various cells, appendages, and the ECM. The balance of traction is thought to contribute to the formation of a

Table 1
Measurement of normal facial muscle strength [93].

Method	Measurement site	Muscle strength (in pounds)
Surface adhesion technique	Eyebrows	0.758
	Eyes	0.549
	Wrinkles	0.387
	Smiles	0.307
Direct probe application	Eyebrows	0.773
	Eyes	0.880
	Smiles	0.730

strong and flexible physical structure that maintains its integrity and flexibility [90]. In addition, the skin accompanies the different movements of the body, subject to a certain degree of mechanical constraints [91]. Moreover, tension contributes to the aging process, which has been the hottest topic apart from cancer research.

3.2.1. Skin mechanical properties

The skin has a complex multi-layered structure composed of non-homogeneous, nonlinear, viscoelastic, anisotropic materials and is subject to *in vivo* pretension [92]. The methods to measure skin tension in human body can be divided into two types: direct measurement of skin tension and detection of elastic modulus. Neely and Pomerantz [93] applied force transducers at the central brow and commissure during eyebrow raising, lid closing, smiling, and frowning, measured by surface adhesion and direct probe application. Measured muscle strength and the results are shown in Table 1.

Kim *et al.* [94] installed a custom-made plastic bridge instrument to provide isometric resistance to skin movement during muscle contraction to quantify the isometric force of the muscles. Agache *et al.* [95] measured the mechanical properties of dermis *in vivo* by applying torque on the skin. Skin mechanical properties of different aging groups, including immediate and delayed viscoelastic components, and corrected raw values for constant skin thickness were evaluated. Subsequently, Hara *et al.* [96] also tested timely deformation, delayed deformation, final deformation, immediate shrinkage, final shrinkage, and residual deformation. However, there are differences in the elastic moduli measured in the literature. The specific values of skin elastic modulus and skin thickness measured in the literature are summarized in Table S6 (Supporting information).

3.2.2. Forces applied in vitro models

(1) Cyclic stress

Oh *et al.* [97] performed cyclic stretching at the frequency of 0.5 Hz on a skin model. The amplitude of the strain varies in the range of 5%−20%. The changes in Interleukin-6 (IL-6) were detected, and it was found that the IL-6 produced by HaCaTs was related to the degree of stretching. Cells induced by mechanical stretching showed higher levels of IL-6 production compared to unstretched cells. IL-6 production was increased by 1.2-fold and 1.3-fold with 5% and 10% stretching, respectively, however, the production of IL-6 levels increased only 1.1-fold with 20% stretching compared to unstretched. It shows that the anti-inflammatory effect is the best when stretched by 10%. In addition, cells were stained and it was found that mechanical stretching induced cytoskeleton remodeling, which changed cell morphology.

Pietramaggiori *et al.* [98] applied a rubber band to the rat ear to form a tension of 0.50 N, and compared the effects of static tension and cyclic tension on the formation of dermal blood vessels. The results showed that after 4 days of continuous tension, the proliferation of epidermal cells increased 4-fold, dermal blood vessels increased 2.8-fold, reaching a peak after 2 days. Using the cyclic loading scheme, a similar effect can be achieved in just 8 h. It shows that applying cyclic stress can better promote cell proliferation.

Peters *et al.* [99] applied cyclic mechanical tension in a sinusoidal mode (0.1 Hz, 24 h), resulting in a maximum biaxial increase of 15% in surface area. In the experimental setup, FBs were seeded on a 6-well collagen I-coated Bioflex plate, with a flexible silicon membrane as the bottom, and the membrane was stretched by repeated vacuuming of the lower chamber. The results showed that down-regulation of mechanical stress-induced endothelin-1 (ET-1), α-smooth muscle actin (αSMA) and connective tissue growth factor (CTGF) expression were found, but the TGFb1 expression was not down regulated. Rolin *et al.* [100] applied cyclic tension in a mode of 10% deformation and 1 Hz, resulting in an increased synthesis of type I procollagen, TIMP-1 and decreased synthesis of MMP-1, indicating that mechanical tension leads to dermal fibroblast differentiation, and may increase its wound healing ability.

(2) Vibration

Caberlotto *et al.* [101] evaluated the effects of different frequencies of vibrational stimulation on a full-skin model. Different explants were used at frequencies of 40, 60, 90 and 120 Hz. It was found that the amounts of laminin 5, collagen 7, collagen type IV markers and perlecan were significantly increased after treatment at 60 Hz, 90 Hz and 120 Hz compared to the untreated control indicating enhanced DEJ. In the dermis, fibronectin markers were significantly increased not only by 60 Hz treatment, but also by 90 Hz treatment, especially in the papillary dermis. Increased expression of procollagen 1 and tropoelastin was also observed.

3.2.3. SOC with mechanical stimuli

Wahlsten *et al.* [102] proposed a novel dynamic bioreactor system for skin tissue that allows exposure of FB-containing collagen hydrogels to pressure-controlled cyclic membrane expansion, in which equibiaxial and uniaxial strains were generated. The results showed that cyclic deformation resulted in hardening of the dermal matrix and stimulated rapid proliferation of FBs, but did not affect the differentiation of FBs into myofibroblasts. Varone *et al.* [10] designed a new comprehensive 3D cell culture system based on the OOC with the advantages offered by 3D organotypic culture. Using microfabrication techniques, a flexible chip consists of a chamber containing organotypic epithelium surrounded by two vacuum channels that can withstand negative vacuum pressure to deform its walls resulting in a simple stretch. The vacuum pressure was adjusted to modify the stretching frequency in the range of 0.01–0.5 Hz, and the strain range was 0−15% leading to a dynamic stretching/relaxing cyclic stress of 90 kPa. In addition, Lim *et al.* [103] designed a wrinkled skin-on-a-chip (WSOC) as shown in Fig. 1. Two layers of PDMS were prepared separately, and permanent magnets were inserted into the cavities between the PDMS layers. Using the attractive and repulsive forces between electromagnets and permanent magnets to unidirectionally stretch gel-containing cells on a chip. On exposure to air and stretching at 0.01 or 0.05 Hz for 12 h at 10% strain for 7 days, wrinkles were found to be formed in the skin equivalent. It was also found that more wrinkles appeared when uniaxially stretched at 0.01 Hz.

4. Applications of SOC

4.1. Drug development

Lukacs *et al.* [57] developed a SOC for *in vitro* monitoring of particle penetration through skin barrier. In their study, tape-stripped and non-stripped skins were studied in parallel for permeability. In comparison with data gained from the traditional Franz cell experiments, their device provided similar results on the absorption of the test drug (caffeine) through dermal barrier. Tarnoki-Zach *et al.* [104] developed a skin model that mimics the epider-

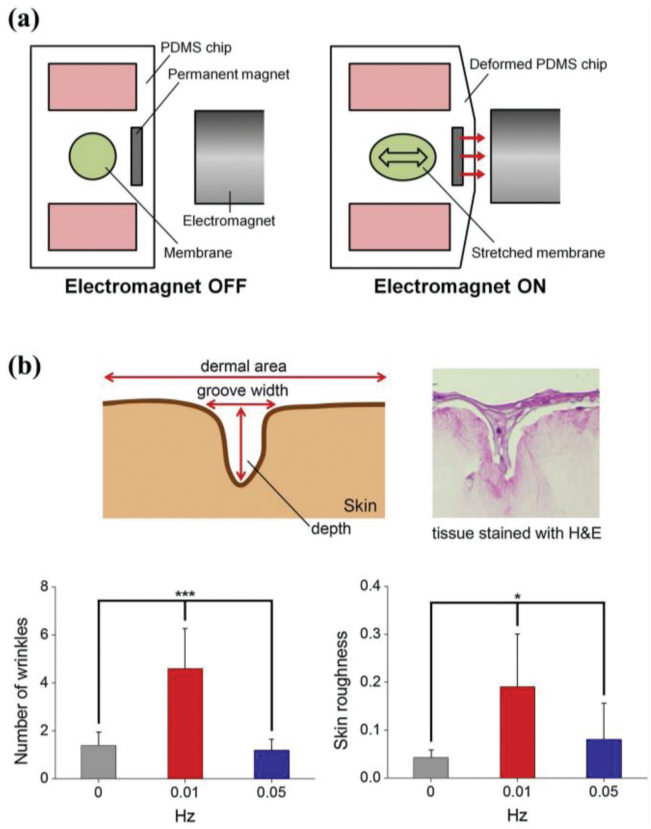

Fig. 1. Wrinkled WSOC. (a) WSOC schematics. (b) The skin wrinkles at different frequencies. Reproduced with permission [103]. Copyright 2018, Elsevier.

mis and connective tissue of the dermis. To provide mechanical integrity suitable for experimental manipulations, they cultured the KCs on the upper surface of an electrospun polycaprolactone (PCL) mesh for the first time, coated with fibronectin. In caffeine concentration diffusion experiments, the skin equivalents exhibited similar concentration changes to native human skin. In addition, Bajza *et al.* [105] used skin chips to determine the skin permeability of quinidine and erythromycin in the presence or absence of the two drugs, and tested the function of skin chips in the interaction between transdermal drug delivery and transporters at skin barrier.

Abaci *et al.* [106] developed a microfluidic chip that allows long-term maintenance of full-thickness HSE. The chip allows blood to have a physiological residence time in the tissue so that the concentration curve of the drug in the blood can be obtained after local administration. At the same time, adriamycin was tested to verify the ability of the platform for drug testing purpose. Mori *et al.* [107] proposed a SOC with vascular channels in order to maintain the permeation of tested drug molecules, caffeine and isosorbide dinitrate, and perfusion conditions promoting percutaneous absorption, which was beneficial to the development and screening of drugs.

Wagner *et al.* [58] integrated human skin biopsy and human primary hepatocytes into a chip to form a multi-organ microfluidic device. The stability can be maintained upto 28 days, and the response of toxic substance troglitazone to liver can be repeatedly tested at different molecular levels. Tavares *et al.* [108] combined the reconstructed human skin (RHS) with the liver model to evaluate the toxicity of exogenous metabolites, and compared with the single RHS cultured under static conditions. Secondary toxicity involved in skin irritation is also provided in microphysical coculture systems.

Provin *et al.* [109] integrated culturing chamber and on-line optical sensors into microfluidic devices. The diffusion curves of seven drugs and nanoparticles were analyzed in order to treat local skin diseases. It was found that the nanoparticles can enhance the permeability and transport efficiency of the skin, which can realize the treatment of local skin diseases.

4.2. Cosmetics testing

Owing to the numerous merits such as cost-effective, low sample consumption, SOC has been fast developing and widely applied in cosmetic testing in terms of ingredient screening and evaluation of skin care products, *etc.* The anti-inflammation tests were the major application of SOC. Kim *et al.* [110] tested the efficacy of natural turmeric leaf extract (CLLE). The results showed that 50 mg/mL CLLE treatment gave the best recovery of skin and thus could be employed in the prevention of aging. The antioxidant effectiveness of α-lipoic acid was also tested [111]. The result showed that α-lipoic acid, as an antioxidant, aids in skin composition, protects the skin such as by forming a barrier to external bacteria, and regulates water, nutrients. Jusoh *et al.* [61] proposed a new *in vitro* skin-irritation platform based on angiogenesis responses induced by VEGF upregulation from damaged KCs as an alternative to animal models.

Lim *et al.* [103] developed an aged skin equivalent using the rapid uniaxial stretching on a perfused co-culture of human KCs and FBs. Wrinkles formed on the skin equivalent and the SC became thinner when stretching was applied. The aging phenomenon in the skin equivalent was further evaluated by visualizing ECM proteins. Their model can be used to test the effect of anti-wrinkle ingredients and cosmetics prior to *in vivo* experiments. Kim *et al.* [112] cultivated HSE with a pump-free skin chip, and adjusted the concentration of coenzyme Q10 in the medium to test its efficacy. Coenzyme Q10 can protect skin from reactive oxygen species (ROS) damage and reduce ultraviolet-induced inflammation.

4.3. Diseases models and wound healing process

Kim *et al.* [113] employed a full-thickness human microscopic skin tissue column (MSTC) to study the neutrophil responses to bacterial infections using SOC with a drop of whole blood as the source of neutrophils without an isolation process. This platform can also be used to test the efficiency of antibiotic treatment. Biglari *et al.* [114] developed a simple wound-on-chip model to assess the effect of an active compounds on wound healing, specifically the inflammation phase that plays a key role in acute and chronic wounds. Incorporation of M1 and M2 macrophages cocultured with FBs and HUVECs led to a stimulation of cytokine production as well as vascular structure formation. The results demonstrated anti-inflammatory effect of dexamethasone. Bogaard *et al.* [115] reported on the successful population of 3D skin equivalents with activated CD4 T cells, Th1 and Th17-polarized T cells. These T-cell subsets and the cytokines are strongly associated with psoriasis pathology. The epidermal inflammation as exemplified by the induced expression of psoriasis-associated marker genes DEFB4 were observed.

Jeon *et al.* [116] conducted drug toxicity experiments on 3D human skin equivalents to study the skin side effects of sorafenib. According to the air exposure time and the concentration of sorafenib anti-cancer agent added to the medium, the changes of equivalents were studied, and the results were compared with the histological results obtained from patients with hand-foot diseases caused by the actual side effects of sorafenib. The thickening of granules and proteins expressed through the change of particle layer were observed to form tissues similar to those of the actual patients, which reproduced the side effects shown in clinic.

The therapeutic effect of 3D bioprinted artificial skin was also evaluated [113,117]. The chimney model simulating the healing process of human wounds was used to analyze the therapeutic effect of the skin models, which can prevent wound contraction. It was found that when FBs and KCs were transplanted, the infiltration rate of wound cells in the dECM transplantation group was faster than that in the control group. In addition, the mice treated with these two cells showed effective collagen deposition in the wound area. The immune response and reepithelialization test also showed that macrophages aggregated to the wound site were much earlier than that of the untreated group, and also higher expression of cytokeratin 14 and Ki67 staining confirmed epidermal regeneration.

Wufuer *et al*. [55] developed a vascularized skin model using a three-layer SOC as dermis wound model to study the wound healing process. The therapeutic effect of dexamethasone (Dex) on reducing TNF-α induced inflammation and edema were tested. Kim *et al*. [118] first reported a diabetic skin platform using 3D bioprinting technology and microfluidic technology. This platform can create a 3D wounded diabetic skin model, which can reproduce delayed wound healing *in vitro* with enhanced diabetes by inducing hyperglycemia and perfusion chamber. The diabetic skin models including insulin resistance, fat cell hypertrophy, inflammation and vascular dysfunction were obtained. In addition, the feasibility of diabetes-related drug screening was also verified using this platform.

5. Limitations and future perspectives

5.1. Limitations in fabrication methods

Bioprinting is a fast fabrication method compared to manual ones and can achieve high-throughput printing with good plasticity and ductility, in particular suitable for skin model fabrication, which has distinguished stratified features, with high repeatability and flexibility [103,119]. Cosmetics and drug screening are included for specific patients as new alternatives to skin transplantation for the treatment of burns and wounds [120], or develop personalized therapy for skin diseases.

Although 3D bioprinting has numerous merits, it is still underdeveloped. Due to the high complexity of the whole system, there is no way to operate production at a large scale. Another challenge for skin bioprinting is to develop large area of skin with highly developed vascular system. Although recent researches have constructed prevascularization models or multi-scale vascular networks with dendritic channels [120]. However, compared with natural skin vessels these are still different. The newly developed ultrafast laser (UL) microfabrication technique might offer the solution. The ultrafast lasers such as femtosecond lasers and picosecond lasers have ultrashort pulse widths and extremely high peak intensities, which provides several unique advantages for advanced material processing, such as suppression of heat-affected zones, maskless surface microprocessing, sub-diffraction-limit nanoablation, highly flexible 3D fabrication in transparent materials, and multifunctional monolithic integration [121–124]. Lin *et al*. [121] applied the UL microfabrication technique to manufacture 3D freeform microfluidic circuits with high aspect ratios in large-scale micro-objects. In their work, centimeter-scale biomimetic hands with surface microreliefs and internal microvasculatures were simultaneously created through ultrafast laser-assisted subtractive printing. Therefore, the ultrafast laser microfabrication holds great potential for constructing large-scale and high-fidelity skin tissues with multi-scale vasculatures in the future [123,125].

The skin models created by 3D bioprinting technology is not yet mature in terms of the printing procedure and the bioinks used for safety concerns, although there are already handhold 3D printers used in the clinics for rapid skin tissue recovery, the 3D bioprinted SEs should be thoroughly tested before the clinic use in the future.

SOC technology, which takes the advantages offered by microfluidics, could be used to culture skin tissues with more reliable functions. The current research on skin models cultured on SOC mainly focuses on the improvement of skin substitutes and the improvement of culture conditions. For the improvement of skin substitutes, enriching the skin structure layer, introducing vascular system and immune system are the main directions, which is directly related to the main application of skin chips, in cosmetic testing and pharmaceutical research.

5.2. Limitations of the current skin models

Although 3D skin models have been fast developing in recent years, there is still a lack of scaling laws to transfer the results from the skin models to *in vivo* tests in particular, in the SOC platforms. The transfer of index of liver function from liver-on-a-chip (LOC) to human scale came to view only recently [126]. In this work, different cultures of hepatocytes and non-solid cells *in vitro* with regulated fluid flow were studied for the oxygen gradient and metabolic partition of toxicity in specific regions to predict drug-induced liver damage in an attempt to access drug safety on LOC. However, the inconsistency between microchip optimization and performance results in these models urgently requires the critical baseline for pharmaceutical industry applications, the commonly accepted scaling law is still underdeveloped.

There is no standard for 3D skin model creation, including cell source, cell type and culturing time. For example, although the microfluidic channels of vascular-like structures [112] allows for the perfusion of nutrition to simulate the blood flow in skin tissues in the aim to improve functions of skin, there is still no commonly accepted knowledge in terms of the perfusion rate on the maturity of skin tissues. Especially, with the fast development of 3D bioprinting techniques, the standards in terms of the preparation methods with living cells involved are still lag behind. In addition, the materials used in skin chips should be evaluated for long term. For instance, PDMS is the most commonly used material at present, but PDMS absorbs small hydrophobic molecules. Therefore, the use of the skin chips in the studies of specific drug toxicity is limited. When the drug is absorbed by PDMS, the actual concentration of the drug is lower, which may underestimate its potential toxicity [3].

At present, there is still a long way to go to mimic the complex structure of living skin. Skin appendages need to be added, including the introduction of microvasculature, immunity, hair follicles, sweat glands and sebaceous glands, pigmentation, subcutaneous inflammation and innervation [50]. In addition, intercellular lipids in SC, such as ceramide (CER), free fatty acid (FFA) and cholesterol (CHOL), contribute to the formation of a stable layered structure in SC, making it important for skin barrier function. Kage *et al*. [127] treated 3D cultured epidermis with GalCer to promote the production of CER, which affects the production of intercellular lipids in SC and improve skin barrier function. However, due to different SC lipids and different barrier permeability, the barrier characteristics of skin models are different from that of natural human skin.

6. Conclusions

In now days, the demand for fully functional 3D skin models has been increased dramatically due to the improved living standard and the booming of beauty industries. The 3D skin models have been fast-evolving owing to the advances of 3D bioprinting

technology, and SOC, in particular. In this review, the skin models produced with these two technologies were evaluated including the newly developed fabrication methods, and the materials used. The functions of the 3D skin models such as the skin barrier, mechanical properties, and the applications were reviewed in detail. The limitations and perspectives in the fabrication methods and the current skin models were also discussed.

SOC and 3D bioprinting are collaborative technologies to create 3D skin models, however there is still a knowledge gap between the 3D skin models and native skin tissue in human, see the above discussion on the limitations. To overcome the limitation of fabrication technology, laser-based printing methods such as UL might offer the possibility to create large skin tissues with micro-vasculatures of multi-scales. To overcome the limitation of the current skin model, the idea is that 3D bioprinting combined with SOC might create native-like fully functioning skin tissues including necessary appendages. The urgent need in the current 3D skin model is to establish the standard of creating 3D skin models and scaling law transferring the testing results from skin models and SOC to human level, it might require the collaborations from multiple sectors such as regulatory authorities, research institutions, and industries.

There may be an interesting future work on building an engineering system by learning the skin function, such as the skin-based sensor for collaborative robots. Another future work may be directed to the study of the robustness and resilience of SOC, as in a general system that has two layers: infrastructure (*e.g.*, chips) and substances (*e.g.*, cells) as well as resilience and robustness in the context of robotic systems [128,129]. The idea is to learn the concept of robustness and resilience of engineering systems to biological systems [130,131].

Declaration of competing interest

The authors declare that they have no known competing financial interests or personal relationships that could have appeared to influence the work reported in this paper.

Supplementary materials

Supplementary material associated with this article can be found, in the online version, at doi:10.1016/j.cclet.2022.107819.

References

[1] European Commission, Regulation (EC) No 1223/2009 of the European Parliament and of the Council, 2009.
[2] L. Broek, L. Bergers, C. Reijnders, S. Gibbs, Stem Cell Rev. 13 (2017) 1–12.
[3] S. Syama, P.V. Mohanan, Trends Food Sci. Technol. 110 (2021) 711–728.
[4] F. Kurth, E. Györvary, S. Heub, et al., Chapter 3 - Organs-on-a-chip engineering, in: J. Hoeng, D. Bovard, M.C. Peitsch (Eds.), Organ-on-a-chip, Academic Press, 2020, pp. 47–130.
[5] D.E. Ingber, Nat. Rev. Genet. 23 (2022) 467–491.
[6] M. Rothbauer, D. Wartmann, V. Charwat, P. Ertl, Biotechnol. Adv. 33 (2015) 948–961.
[7] D. Huh, G.A. Hamilton, D.E. Ingber, Trends Cell Biol. 21 (2011) 745–754.
[8] S.E. Park, A. Georgescu, D. Huh, Science 364 (2019) 960–965.
[9] J. Kelm, R. Marchan, Arch. Toxicol. 88 (2014) 1913–1914.
[10] A. Varone, J.K. Nguyen, L. Leng, et al., Biomaterials 275 (2021) 120957.
[11] J. Zhang, Z. Chen, Y. Zhang, et al., Lab Chip 21 (2021) 3804–3818.
[12] H. Si, T. Xing, Y. Ding, et al., Polymers 11 (2019) 1584.
[13] T. Wang, J. Zheng, T. Hu, H. Zhang, W. Zhang, 3D Print. Addit. Manuf. 8 (2021) 1–13.
[14] Ž. Kačarević, P. Rider, S. Alkildani, et al., Materials 208 (2021) 112041.
[15] C. Gao, C. Lu, Z. Jian, et al., Colloids Surf. B 208 (2021) 112041.
[16] S.V. Murphy, A. Atala, Nat. Biotechnol. 32 (2014) 773–785.
[17] M. Askari, M.A. Naniz, M. Kouhi, et al., Biomater. Sci. 9 (2021) 535–573.
[18] X. Chen, L. Ning, Biotechnol. J. 12 (2017) 1600671.
[19] A. Blaeser, D.D. Campos, U. Puster, et al., Adv. Healthc. Mater. 5 (2016) 326–333.
[20] A.N. Leberfinger, D.J. Ravnic, A. Dhawan, I.T. Ozbolat, Stem Cell Transl. Med. 6 (2017) 1940–1948.
[21] H. Gudupati, M. Dey, I. Ozbolat, Biomaterials 102 (2016) 20–42.
[22] J.Y. Park, J. Jang, H.W. Kang, Microelectron. Eng. 200 (2018) 1–11.
[23] E. Tekin, P.J. Smith, U.S. Schubert, Soft Matter 4 (2008) 703–713.
[24] B. Zhang, Y. Luo, M. Liang, et al., Bio Des. Manuf. 1 (2018) 2–13.
[25] Luo Y.X, X. Lin, P. Huang, Macromol. Biosci. 18 (2018) 1800034.
[26] Z. Gu, J. Fu, H. Lin, Y. He, Asian J. Pharm. Sci. 15 (2020) 529–557.
[27] T. Billiet, M. Vandenhaute, J. Schelfhout, S. Van Vlierberghe, P. Dubruel, Biomaterials 33 (2012) 6020–6041.
[28] J. Adhikari, A. Roy, A. Das, et al., Macromol. Biosci. 21 (2021) e2000179.
[29] A. Hoffmann, H. Leonards, N. Tobies, L. Pongratz, N. Nottrodt, J. Tissue Eng. 8 (2017), doi:10.1177/2041731417744485.
[30] S.H. Kim, Y.K. Yeon, J.M. Lee, et al., Nat. Commun. 9 (2018) 1620.
[31] J. Jang, J.Y. Park, G. Gao, D.W. Cho, Biomaterials 156 (2018) 88–106.
[32] Y.B. Lee, S. Polio, W. Lee, et al., Exp. Neurol. 223 (2010) 645–652.
[33] W. Lee, V. Lee, S. Polio, et al., Biotechnol. Bioeng. 105 (2010) 1178–1186.
[34] V. Lee, G. Singh, J.P. Trasatti, et al., Tissue Eng. Part C: Methods 20 (2014) 473–484.
[35] S. Ramasamy, P. Davoodi, S. Vijayavenkataraman, et al., Bioprinting 21 (2021) e00123.
[36] R.E. Burgeson, A.M. Christiano, Curr. Opin. Cell Biol. 9 (1997) 651–658.
[37] S. Jin, Y.N. Oh, Y.R. Son, et al., J. Microbiol. Biotechnol. 32 (2022) 238–247.
[38] A.F. Deyrieux, V.G. Wilson, Cytotechnology 54 (2007) 77–83.
[39] M. Akiyama, T. Takeichi, J.A. Mcgrath, K. Sugiura, J. Allergy Clin. Immunol. 112 (2017) 1545–1547.
[40] D. Hohl, B.R. Olano, P.A. de Viragh, et al., Differentiation 54 (1993) 25–34.
[41] B.S. Kim, Y.W. Kwon, J.S. Kong, et al., Biomaterials 168 (2018) 38–53.
[42] M.D. Nordlund, J. James, Dermatol. Clin. 25 (2007) 271–281.
[43] W.L. Ng, J.T.Z. Qi, W.Y. Yeong, et al., Biofabrication 10 (2018) 025005.
[44] L. Shi, L. Xiong, Y. Hu, et al., Polym. Eng. Sci. 58 (2018) 1782–1790.
[45] H.I. Choi, K.C. Sohn, D.K. Hong, Y. Lee, Y.H. Lee, Arch. Dermatol. Res. 306 (2014) 59–66.
[46] M. Mehling, S. Tay, Curr. Opin. Biotechnol. 25 (2014) 95–102.
[47] Q. Zhang, L. Sito, M. Mao, et al., Microphysiol. Syst. 2 (2018) 50–57.
[48] K.S. Nitsche, I. Muller, S. Malcomber, P.L. Carmichael, H. Bouwmeester, Arch. Toxicol. 96 (2022) 711–741.
[49] E. Sutterby, P. Thurgood, S. Baratchi, K. Khoshmanesh, E. Pirogova, Small 16 (2020) e2002515.
[50] M. Cui, C. Wiraja, M. Zheng, et al., Adv. Ther. 5 (2021) 2100138.
[51] V. Faustino, S.O. Catarino, L. Rui, E.G. Minas, J. Biomech. 49 (2015) 2280–2292.
[52] R.M. Kiran, S. Chakraborty, J. Appl. Polym. Sci. 137 (2020) 48958.
[53] Q. Ramadan, F.C. Ting, Lab Chip 16 (2016) 1899–1908.
[54] N. Sasaki, K. Tsuchiya, H. Kobayashi, Sens. Mater. 31 (2019) 107–115.
[55] M. Wufuer, G. Lee, W. Hur, et al., Sci. Rep. 6 (2016) 37471.
[56] B. Atac, I. Wagner, R. Horland, et al., Lab Chip 13 (2013) 3555–3561.
[57] B. Lukacs, A. Bajza, D. Kocsis, et al., Pharmaceutics 11 (2019) 445.
[58] I. Wagner, E.M. Materne, S. Brincker, et al., Lab Chip 13 (2013) 3538–3547.
[59] I. Maschmeyer, A.K. Lorenz, K. Schimek, et al., Lab Chip 15 (2015) 2688–2699.
[60] H.J. Song, H.Y. Lim, W. Chun, et al., J. Ind. Eng. Chem. 56 (2017) 375–381.
[61] N. Jusoh, J. Ko, N.L. Jeon, APL Bioeng. 3 (2019) 036101.
[62] S. Salameh, N. Tissot, K. Cache, et al., Biofabrication 13 (2021) 035042.
[63] S. Lee, S.P. Jin, Y.K. Kim, et al., Biomed. Microdevices 19 (2017) 22.
[64] K. Takahashi, S. Yamanaka, Cell 126 (2006) 663–676.
[65] K. Gledhill, Z. Guo, N. Umegaki-Arao, et al., PLoS One 10 (2015) e0136713.
[66] I. Risueño, L. Valencia, M. Holgado, J.L. Jorcano, D. Velasco, JoVE J. Vis. Exp. 171 (2021) e62353.
[67] G. Sriram, M. Alberti, Y. Dancik, et al., Mater. Today 21 (2018) 326–340.
[68] J. Yeste, X. Illa, M. Alvarez, R. Villa, J. Biol. Eng. 12 (2018) 18.
[69] T. Montero-Vilchez, M.V. Segura-Fernández-Nogueras, I. Pérez-Rodríguez, et al., J. Clin. Med. 10 (2021) 359.
[70] C.Y. Hsu, N. Lecland, V. Pendaries, et al., J. Dermatol. Sci. 91 (2018) 87–96.
[71] V. Planz, C.M. Lehr, M. Windbergs, J. Control. Release 242 (2016) 89–104.
[72] B. Srinivasan, A.R. Kolli, M.B. Esch, et al., J. Lab Autom. 20 (2015) 107–126.
[73] C. Shuai, E. Ralf, S. Jennifer, Histochem. Cell Biol. 144 (2015) 509–515.
[74] P. Zoio, S. Lopes-Ventura, A. Oliva, Micromachines 12 (2021) 816.
[75] E. Toulza, N.R. Mattiuzzo, M.F. Galliano, N. Jonca, Genome Biol. 8 (2007) R107.
[76] E. Guttman-Yassky, M. Suárez-Fariñas, A. Chiricozzi, et al., J. Allergy Clin. Immunol. 124 (2009) 1235–1244.
[77] K. Bäsler, S. Bergmann, M. Heisig, et al., J. Control. Release 242 (2016) 105–118.
[78] K. Murakami, A. Sawada, T. Mori, S. Sakuyama, Y. Tokudome, Life Sci. 293 (2022) 120356.
[79] M. Murakami, T. Akagi, Y. Sasano, et al., J. Tissue Eng. Regen. Med. 15 (2021) 798–803.
[80] T. Kubo, S. Sato, T. Hida, et al., Immun. Inflamm. Dis. 9 (2021) 734–745.
[81] T.J. Pell, M.B. Gray, S.J. Hopkins, et al., SLAS Discov. 26 (2021) 909–921.
[82] Y. Uchida, A. Celli, A method to investigate the epidermal permeability barrier *in vitro*, Methods in Molecular Biology, Clifton, 2020, pp. 73–90.
[83] S.J. Bashir, A.L. Chew, A. Anigbogu, F. Dreher, H.I. Maibach, Skin Res. Technol. 7 (2010) 40–48.
[84] M. Denzinger, J. Rothenberger, M. Held, et al., J. Tissue Viability 28 (2019) 194–199.
[85] P.W. Wertz, Semin. Dermatol. 11 (1992) 106–113.
[86] M.C. Martini, Pathol. Biol. 51 (2003) 267–270.
[87] N. Amen, D. Mathow, M. Rabionet, et al., Hum. Mol. Genet. 22 (2013) 4164–4179.
[88] I.M. Dijkhoff, B. Petracca, R. Prieux, et al., JoVE J. Vis. Exp. 171 (2021) e61802.

[89] P. Zoio, S. Lopes-Ventura, J. Marto, A. Oliva, ALTEX Altern. Anim. Exp. 39 (2022) 405–418.
[90] S. Kimura, A. Tsuchiya, M. Ogawa, et al., Commun. Biol. 3 (2020) 637.
[91] C. Escoffier, J.D. Rigal, A. Rochefort, et al., J. Invest. Dermatol. 93 (1989) 353–357.
[92] G. Boyer, J. Molimard, M.B. Tkaya, et al., J. Mech. Behav. Biomed. 27 (2013) 273–282.
[93] J.G. Neely, R.G. Pomerantz, Laryngoscope 112 (2002) 1562–1568.
[94] K.E. Kim, S.H. Oh, S.U. Lee, S.G. Chung, Clin. Biomech. 24 (2009) 606–612.
[95] P.G. Agache, C. Monneur, J.L. Leveque, J.D. Rigal, Arch. Dermatol. Res. 269 (1980) 221–232.
[96] Y. Hara, Y. Masuda, T. Hirao, N. Yoshikawa, Skin Res. Technol. 19 (2013) 339–345.
[97] S. Oh, H. Chung, S. Chang, et al., Sci. Rep. 9 (2019) 5156.
[98] G. Pietramaggiori, P. Liu, S.S. Scherer, et al., Ann. Surg. 246 (2007) 896–902.
[99] A.S. Peters, G. Brunner, K. Blumbach, et al., Exp. Dermatol. 21 (2012) 765–770.
[100] G.L. Rolin, D. Binda, M. Tissot, et al., J. Biomech. 47 (2014) 3555–3561.
[101] E. Caberlotto, M. Bernal, Z. Miller, et al., Skin Res. Technol. 25 (2019) 881–889.
[102] A. Wahlsten, D. Rutsche, M. Nanni, et al., Biomaterials 273 (2021) 120779.
[103] H.Y. Lim, J. Kim, H.J. Song, et al., J. Ind. Eng. Chem. 68 (2018) 238–245.
[104] J. Tarnoki-Zach, E. Mehes, Z. Varga-Medveczky, et al., Pharmaceutics 13 (2021) 910.
[105] A. Bajza, D. Kocsis, O. Berezvai, et al., Pharmaceutics 12 (2020) 804.
[106] H.E. Abaci, K. Gledhill, Z. Guo, A.M. Christiano, M.L. Shuler, Lab Chip 15 (2015) 882–888.
[107] N. Mori, Y. Morimoto, S. Takeuchi, Biomaterials 116 (2017) 48–56.
[108] R.S.N. Tavares, T.P. Tao, I. Maschmeyer, et al., Int. J. Pharm. 589 (2020) 119788.
[109] C. Provin, A. Nicolas, S. Grégoire, T. Fujii, Pharm. Res. 32 (2015) 2704–2712.
[110] K. Kim, H.M. Jeon, K.C. Choi, G.Y. Sung, Int. J. Mol. Sci. 21 (2020) 3898.
[111] K. Kim, J. Kim, H. Kim, G.Y. Sung, Int. J. Mol. Sci. 22 (2021) 2160.
[112] J. Kim, K. Kim, G.Y. Sung, Int. J. Mol. Sci. 21 (2020) 8475.
[113] J.J. Kim, F. Ellett, C.N. Thomas, et al., Lab Chip 19 (2019) 3094–3103.
[114] S. Biglari, T.Y.L. Le, R.P. Tan, et al., Adv. Healthc. Mater. 8 (2019) 1801307.
[115] E.H. Bogaard, G.S. Tjabringa, I. Joosten, et al., J. Invest. Dermatol. 134 (2014) 719–727.
[116] H.M. Jeon, K. Kim, K.C. Choi, G.Y. Sung, J. Ind. Eng. Chem. 82 (2020) 71–80.
[117] J. Seo, S.J. Park, J.J. Choi, et al., Wound Repair Regen. 24 (2016) 686–694.
[118] B.S. Kim, M. Ahn, W.W. Cho, et al., Biomaterials 272 (2021) 120776.
[119] G. Gao, X. Cui, Biotechnol. Lett. 38 (2016) 203–211.
[120] W.L. Ng, S. Wang, W.Y. Yeong, M.W. Naing, Trends Biotechnol. 34 (2016) 689–699.
[121] Z. Lin, J. Xu, Y. Song, et al., Adv. Mater. Technol. 5 (2020) 1900989.
[122] P. Wang, W. Chu, W. Li, et al., Micromachines 10 (2019) 565.
[123] K. Sugioka, Y. Cheng, Light Sci. Appl. 3 (2014) e149.
[124] X. Li, J. Xu, Z. Lin, et al., Appl. Surf. Sci. 485 (2019) 188–193.
[125] K. Sugioka, J. Xu, D. Wu, et al., Lab Chip 14 (2014) 3447–3458.
[126] A.R. Baudy, M.A. Otieno, P. Hewitt, et al., Lab Chip 20 (2020) 215–225.
[127] M. Kage, Y. Itaya, J. Horikoshi, Y. Tokudome, Biochem. Biophys. Rep. 28 (2021) 101135.
[128] W.J. Zhang, A. van Luttervel, C.I.R.P. Ann, Manuf. Technol. 60 (2011) 469–472.
[129] F. Wang, Z. Qian, Z. Yan, C. Yuan, W. Zhang, IEEE Access 8 (2020) 2885–2892.
[130] K. Wang, R. Yin, Y. Lu, et al., Mater. Sci. Eng. C 126 (2021) 112185.
[131] C. Yuan, A. Tony, R. Yin, K. Wang, W. Zhang, Sensors 21 (2021) 1234.